2004

The Activity of Silicon Carbide Particles in Al-Based Metal Matrix Composites Revealed by Scanning Electrochemical Microscopy

David O. Wipf
Mississippi State University, dow1@msstate.edu

L. Díaz-Ballote

L. Veleva

M. A. Pech-Canul

M. I. Pech-Canul

Activity of SiC Particles in Al-Based Metal Matrix Composites Revealed by SECM L. Díaz-Ballote *et al* 2004 *J. Electrochem. Soc.* **151** B299 https://doi.org/10.1149/1.1737384

The Activity of Silicon Carbide Particles in Al-Based Metal Matrix Composites Revealed by Scanning Electrochemical Microscopy

L. Díaz-Ballote[a], L. Veleva[*a], M. A. Pech-Canul[*a],
M. I. Pech-Canul[b], and David O. Wipf[*z]

Department of Chemistry, Box 9573, Mississippi State University
Mississippi State, MS 39762, USA

ABSTRACT

Scanning electrochemical microscopy (SECM) is used to image variations in electrochemical activity over the surface of an aluminum-based metal matrix composite (MMC) in contact with buffered or unbuffered neutral solutions. The composite consists of an Al - 13.5% Si - 9% Mg alloy matrix and reinforcing silicon carbide particles (SiC_p). Feedback mode SECM imaging using ferrocenemethanol as a redox mediator in 0.1 M NaCl solution and in buffer solution (pH 6.8) revealed that the SiC particles are electrochemically active. The data suggest that the electronic conductivity at these sites is higher than that of the Al_2O_3 film covering the alloy matrix surface. The reduction of dissolved oxygen on the silicon carbide particles was investigated by *in situ* SECM images of samples and current vs. tip-substrate distance curves. The results with samples of SiC_p/Al composites immersed in distilled water alone or in either 0.1 M NaCl or boric acid/borax buffer containing ferrocenemethanol as mediator demonstrate that the silicon carbide particles are conductive and act as local cathodes for the reduction of oxygen.

Submitted to the *Journal of the Electrochemical Society* June 16, 2003, revised Dec 8, 2003

[a] Applied Physics Department, Center for Investigation and Advanced Study (CINVESTAV-IPN), Unidad Mérida, AP 73 Cordemex, Mérida, Yuc., 97310, México

[b] Center for Investigation and Advanced Study (CINVESTAV-IPN), Unidad Saltillo, Carr. Saltillo-Monterrey Km 13, A.P. 663, Saltillo, Coahuila 25000, México

[*] Electrochemical Society Member

[z] wipf@ra.msstate.edu

INTRODUCTION

The use of aluminum-based metal-matrix composites, MMCs, has attracted considerable attention due to their low density and enhanced mechanical properties compared to conventional structural aluminum alloys. Although different matrix-reinforcement combinations are possible, the combination of commercial aluminum alloys with silicon carbide particles, SiC_p, is one of the most interesting for industrial applications.[1,2]

Al/SiC_p composites have emerged as materials with especially attractive combination of physical properties, manufacturing flexibility, and cost. The composites have low densities and can be formed by stamping. The high volume fraction of the ceramic reinforcement provides high thermal conductivity and allows adjustable thermal expansion coefficients, which makes the composites particularly useful in electronic packaging and in applications where substantial improvement in strength and stiffness, relative to the un-reinforced materials, is required.[3,4] Other uses are found in the aerospace industry and in high-performance automotive applications for brake calipers and cylinder linings.

Al-based MMCs reinforced with SiC_p can be produced by a variety of techniques. One of these is the pressureless infiltration method (infiltration of a reinforcement preform with molten metal), which has not achieved its full technological potential due to a pair of technical difficulties: inadequate wetting of SiC by molten aluminum and interfacial reactions leading to the formation of Al_4C_3. These problems were addressed in a recent study.[5] Determination of optimum process parameters (which optimized wetting and minimized interfacial reactions) included a search for most favorable silicon and

magnesium contents in the alloy (13.5 % Si, 9 % Mg). An investigation of the mechanical properties of the Al-13.5Si-9Mg/SiC_p composite,[5] and a preliminary study of its corrosion behavior in chloride-containing solutions have been reported recently.[6]

The corrosion resistance of MMCs is a vital parameter in assessing their potential application as structural materials. Thus, for Al-based MMCs reinforced with SiC_p, several studies in chloride-containing environments have been reported.[7-13] With few exceptions,[8] the corrosion characteristic of the composites in such environments was mainly localized attack taking place at the reinforcement-matrix interface. Depending on the alloy composition and processing, the origin of the localized attack has been attributed to micro-galvanic coupling between matrix and reinforcement[10-12] or between the matrix and intermetallics,[12] failure of protective oxide film due to microsegregation of alloying elements,[8] and microcrevices at the matrix-reinforcement interface.[10,12]

There seems to be a general agreement that the primary driving force for corrosion in aerated media is the oxygen reduction reaction, however there is disagreement on the localization of the cathodic sites. Some authors ascribed the cathodic sites to the SiC_p,[10,11,13] others to the matrix-reinforcement interface[7,9] or to intermetallic compounds in the matrix alloy.[12] Inherent to this controversy is the role of the reinforcement on the electrochemical behavior of the SiC_p/Al-based MMCs. Conflicting results indicate that the SiC_p are either electrochemically active[10,11,13] or inert.[12] Such apparent contradiction is probably related to the fact that SiC is a semiconductor with electrical resistivities varying from 10^{-5} to 10^{13} Ω–cm, depending on its purity.[13-15] However the problem has not been fully addressed in the literature.

The scanning electrochemical microscope is based on the steady-state current

generated by the electrolysis of an electroactive mediator at a microelectrode (hereafter the tip).[16-18] When the tip is brought close to a conductive surface, an increase in tip current occurs because of the electrolytic regeneration of the mediator at the substrate (i.e. *positive feedback*). However when the tip approaches an insulating surface, tip current decreases because the diffusion of the mediator is blocked (*negative feedback*). This behavior of the steady-state current permits a determination of the local conductivity of the substrate surface. In the more general case, the rate of electron transfer between the mediator and the substrate must also be considered. Very slow electron transfer at a conductive substrate mimics the negative feedback behavior of an insulating surface. Intermediate electron transfer rates (i.e. the "reaction-rate" mode) produce behavior that is a mixture of the negative and positive feedback effects.[19,20]

In addition to the feedback process described above, the SECM can image surfaces in the generation/collection (GC) mode. This mode is used to map the concentration of chemical species produced by a chemical or electrochemical reaction at the substrate. In the amperometric GC mode the tip is set at a potential sufficient to electrolyze a species produced or destroyed at the substrate surface. The tip current is used to produce a map of the chemical concentration. Of particular interest here is the ability of the SECM to directly image oxygen concentration at surfaces.[21-24] Thus, SECM could assist in revealing the electrochemical activity of the SiC particles in SiC_p/Al-based MMCs exposed to neutral aerated media. To our knowledge, such an approach has not been reported so far for examining MMCs. A recent report explores similar concerns for intermetallic inclusions in Cu-containing Al alloys.[25]

The aims of this work are to: determine the distribution and location of

electrochemically active sites in the MMC and to characterize the heterogeneous distribution of oxygen reduction on this surface. These results contribute to the characterization of the corrosion behavior of the Al-13.5Si-9Mg/SiC_p composite in neutral chloride solutions and demonstrate that SECM is a useful technique for investigating the distribution of electrochemical activity on the surface of MMCs.

EXPERIMENTAL PROCEDURE

The composite material used in this investigation was prepared as reported previously.[5,26] A 2 mm × 3 mm sample was potted in EPON 828 epoxy (Miller-Stephenson, Danbury, CT) with 13 % triethylenetetramine hardener (Miller-Stephenson) by weight and was prepared for examination by grinding with 320, 600, and 1500 grit SiC paper and then polished with alumina abrasives down to 0.05 μm. All electrolyte solutions were prepared with reagent grade chemicals and distilled, deionized water (18.2 MΩ-cm). Ferrocenemethanol (97 % purity, Aldrich, Milwaukee WI) was used without further purification.

Imaging tips were 10-μm diam Pt and Au disks, glass insulated and built as described previously by sealing Pt and Au wires (Goodfellow Metals, Ltd., Cambridge, UK) into soft glass.[27,28] In all *x-y* SECM images, the tip was positioned about 3 μm above the substrate and scanned at 20 μm/s parallel to the substrate at a constant height. The tip potential was poised at 600 mV vs. Ag/AgCl for the oxidation of ferrocenemethanol and –400 mV vs. Ag/AgCl for the reduction of the dissolved oxygen. The open circuit potential (*ocp*) of the Al/SiC_p MMC in unbuffered 0.1 M NaCl + 2 mM ferrocenemethanol (pH = 6.8) was about –650 mV vs. Ag/AgCl. In the boric acid/ borax

buffer with 2 mM ferrocenemethanol (pH = 6.8) the *ocp* was –500 mV vs. Ag/AgCl. All potentials are reported vs. the Ag/AgCl reference electrode.

RESULTS AND DISCUSSION

Surface Reactivity Ferrocenemethanol was chosen as a mediator for SECM examination of the conductivity of the Al/SiC_p composite. Ferrocenemethanol shows a reversible cyclic voltammogram with an $E_{1/2}$ of 260 mV vs. Ag/AgCl in 0.1 M NaCl. Therefore we chose a tip voltage of 600 mV to oxidize the ferrocenemethanol at a diffusion controlled rate and to produce a steady-state current. In addition, the *ocp* of the substrate in this solution is –650 mV, more negative than required to reduce the tip-oxidized ferrocenemethanol.

An optical micrograph of the Al/SiC_p composite is shown in Figure 1A. The SiC is embedded in the Al matrix and exists as discrete, light-gray, irregularly shaped particles (c.f. particle marked as 1 in Figure 1A). A SECM image of the same region is shown in Figure 1B. The image was obtained with the composite at open circuit in a solution of 0.1 M NaCl (pH 6.8) and 2 mM ferrocenemethanol. In comparing the SECM and optical micrograph, it is clear that the largest tip currents (> 2 nA) are recorded above the SiC particles and the lower currents are over the Al matrix. This indicates that the SiC is acting as a conductor and reducing the tip-generated oxidized ferrocenemethanol. The Al matrix is acting as an insulator due to the presence of an aluminum oxide film. The optical and SECM images show very good agreement. However, the optical image, acquired after the SECM experiment, shows evidence of corrosion. Pits are clearly seen on the optical micrograph as the dark regions at the right edge, center, and upper left of

the micrograph. Corrosion was also noted during experiments by visible gas bubbles and corrosion products at the substrate surface.

Current vs. distance curves over the particle marked 1 and a portion of the matrix marked 2 (Figures 1A and 1C) show very different feedback behavior. The tip current increases when the tip approaches the particle; an indication of a positive feedback and confirming the conductive nature of the SiC_p.[16]

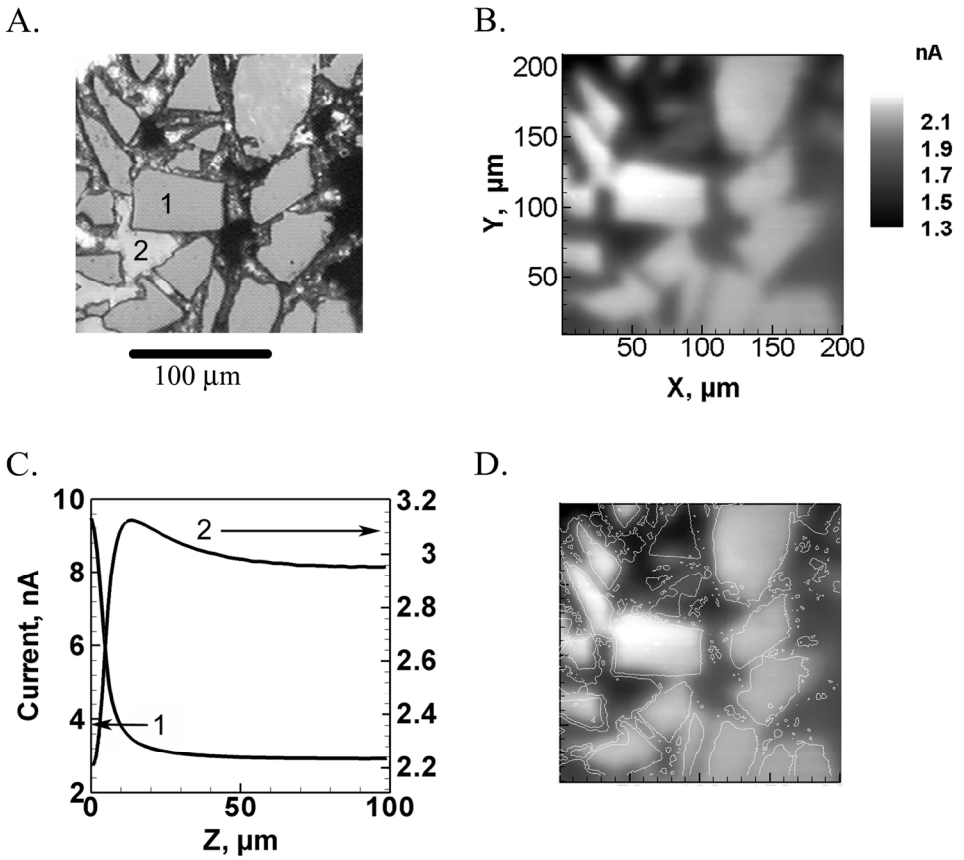

FIGURE 1. Optical (A.) and SECM (B.) images of the SiC_p/Al composite. For the SECM image, the substrate-tip separation was less than 5 µm using a 10 µm diam Au tip biased at 600 mV vs Ag/AgCl. The SECM image was recorded in an aqueous solution of 0.1 M NaCl and 2 mM ferrocenemethanol (pH 6.8). The substrate was at *ocp* (–650 mV vs. Ag/AgCl). (C.) Tip current-distance curves over the regions of image A marked 1 and 2. (D.) Overlay of the SiC particle outlines from the optical micrograph on the SECM image.

The current-distance curve over the Al alloy (Figure 1C) shows behavior that is typical for a mixture of positive and negative feedback. The slight increase in tip current about 20 μm above the alloy and subsequent decrease likely indicates positive feedback from the SiC particles surrounding the Al matrix at larger tip-substrate separation. The greater substrate interaction area at larger tip-substrate separation allows some positive feedback that is eliminated as the tip move closer to the surface. An alternate, but less likely explanation, is that a reaction-rate type process is occurring. This involves a competition between the mediator turnover rate (set by the current density at the substrate) and diffusional blocking by the tip and substrate.[19,20] At larger distances, the tip-generated mediator diffuses laterally a significant amount before interacting with the substrate, this larger interaction area requires a lower current density at the substrate. Closer to the substrate, the effective current density at the substrate must increase to maintain positive feedback, which is not possible. The slow electron-transfer rate constant would be attributed to a non-conducting oxide layer on the aluminum alloy as expected from the stability diagram of aluminum.[29] However, a recent study by Serebrennikova and White applied SECM to investigate the localized electrochemical activity at Al surfaces covered by a 2-3 nm thick native oxide film.[30] Their results indicated that, except for some isolated microscopic defect sites, the nanometer-thick Al_2O_3 film effectively blocks electron transfer between the metal and solution within the imaged area.

An intriguing aspect of the image is that the SiC particles are not uniformly active. This can be appreciated by overlaying the outlines of the SiC particles (generated by a graphics program) on the SECM image (Figure 1D). For example, the three triangular

particles at upper center show low or no feedback response. It is not yet clear why an isolated particle acts differently than its neighbors. An additional aspect is that the SiC particles show less current than expected based on the current-distance curve of Figure 2C. However, we often observed a slow passivation process (over several hours) in this media leading to reduced contrast in the images. It is likely that this passivation was caused by corrosion products from the Al matrix.

Figure 2A shows an SECM image of a composite in a less corrosive boric acid/borax buffer (pH 6.8). Once again, the tip current is higher at the SiC particles, indicating higher conductivity. To further illustrate the heterogeneous behavior of the surface, a series of approach curves were recorded along a line of constant x from $y = 0$ to 180 μm (dashed line). The approach curves are divided into three plots for clarity. Figure 2B shows approach curves at $y = 0$ to 60 μm. An increase in tip current is evident starting around $z = 10$ μm when $y > 10$ μm. This indicates positive feedback behavior at the SiC. Interestingly, the tip current increases to a maximum at around 5 μm and then decreases at closer approach. Unlike the superficially similar behavior seen over the matrix in Figure 1C, the more likely explanation here is a slow electron transfer process at the SiC. We believe that ultimately this results from a partial coverage of the particle by corrosion products originating from the Al matrix since the particle shows a fully realized positive feedback response at $y > 60$ μm (Figure 2C). At distances greater than 100 μm, the approach curves show a negative feedback behavior (Figures Figure 2C and 2D), indicating the tip has moved off of the SiC particle and on to the Al matrix. Notice, however, the curve at $y = 180$ μm decreases more than others. Again the explanation is likely due to the presence of nearby SiC causing a mixed response (*vida supra*).

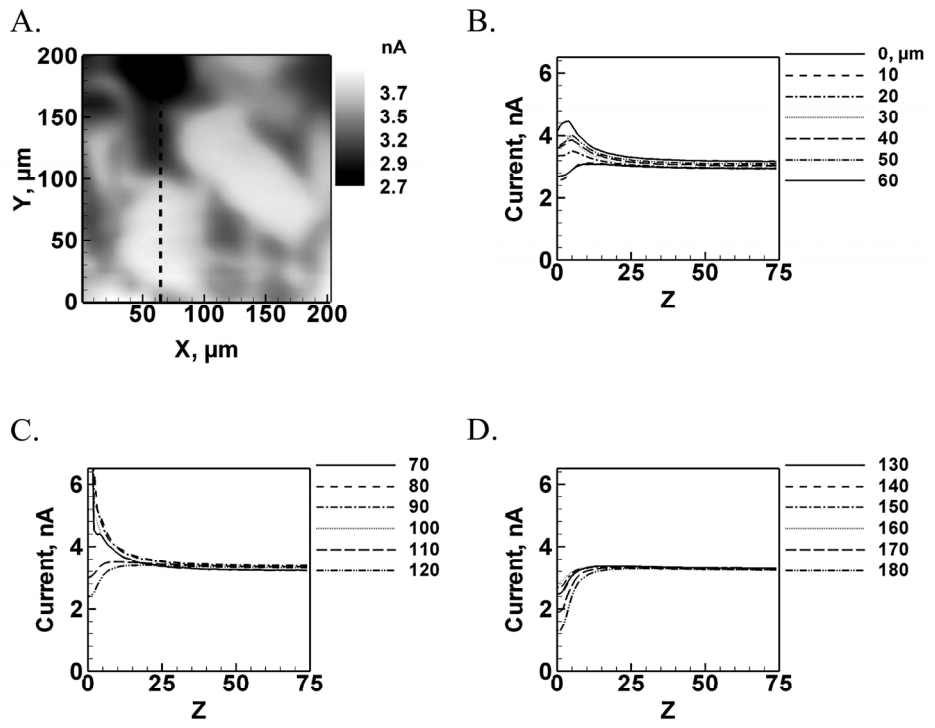

FIGURE 2. SECM image (A.) of the SiC_p/Al composite. The image was obtained with a 10 µm diam Pt tip biased at 600 mV vs Ag/AgCl, and the solution used was boric acid/borax buffer (pH 6.8) containing 2 mM of ferrocenemethanol as a mediator. The substrate was at *ocp* (550 mV vs. Ag/AgCl) during the experiment. (B., C., and D.) Tip current vs substrate-tip distance at different *y* distances (as indicated) along the dashed line in (A.)

Comparison of the SECM image in Figure 2 with the current-distance curves indicates that the SECM image provides a representative image but incompletely describes the nature of the surface. Only the current-distance relationship can clearly distinguish the different types of conductivity seen at this surface

Variation of Oxygen Reduction at the Electrode Surface The conductivity of the SiC particles suggests that, at *ocp*, the SiC in the composite should reduce oxygen and, thus, promote corrosion at the Al matrix. SECM experiments were used to investigate whether oxygen is indeed reduced at the SiC particles.

Oxygen imaging was first performed by adding distilled-deionized water to the cell. Oxygen is readily detected at the tip by the presence of a cathodic current measured at -400 mV. The tip current vs. the tip-substrate distance curve in Figure 3A shows that, as the tip approaches the substrate, the oxygen reduction current decreases. In this case, the current decrease is due to two separate effects: at close distance (< 20 μm) the rapid current drop is due primarily to the negative feedback caused by the substrate physically blocking oxygen diffusion. The more gradual decrease at larger distances is due to the consumption of oxygen by the surface, reducing the concentration of oxygen near the surface. The current-distance behavior in Figure 3A clearly indicates that the unbiased substrate, *ocp* = –490 mV, is able to reduce oxygen at its surface.

The location of oxygen reduction can be identified by SECM imaging. Using current–distance relationships similar to that in Figure 3A, the SECM tip was positioned about 4 μm above the substrate and a scan of the surface was done. The result was the SECM image in Figure 3B. Because this GC image is based on diffusion of material from the surface, a certain amount of blurring occurs and the image is not as resolved as in Figures 1B and 2A. The image indicates that the concentration of oxygen varies significantly over the imaged region. Note that lighter gray indicates the lowest tip current and, thus, lower oxygen concentration. The image is not unambiguous, however, the current may also decrease due to sample topography. A decrease in tip–substrate distance will diminish the oxygen signal by the negative feedback effect (i.e. diffusional blocking). However an initial view indicates that negative feedback is not likely to be the sole contrast mechanism for the image in Figure 3B since the significant blurring is more

typical of a generation/collection image.

Electron transfer from the surface is responsible for the observed diminishment of oxygen at the surface. This can be verified by biasing the composite at more negative potentials where the oxygen reduction is accelerated. Figure 3C shows a set of line scans at the same tip position crossing the sample at x = 25 µm (indicated by the white–dashed line in Figures 3B and 3D) but with the substrate at different potentials. At *ocp*, –490 mV, the line scan is simply a trace of the image data. At slightly more negative

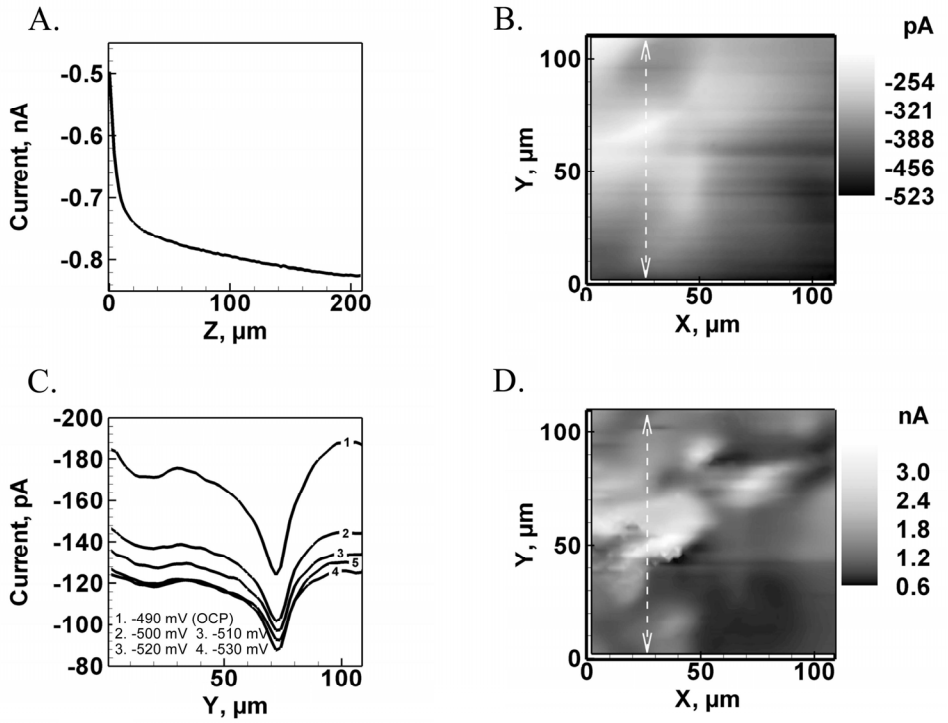

FIGURE 3. (A.) Tip current vs distance curve for oxygen reduction at the SiC_p/Al composite. (B.) Generation/collection image of the oxygen at the SiC_p/Al composite recorded in distilled water. For (A.) and (B.) the tip was a 10 µm diam Pt electrode biased at –400 mV vs Ag/AgCl, (C.) Single line scan data of the oxygen reduction current along the dashed line in figure B. Substrate potential at *ocp* (–490 mV) and biased at potentials as indicated (–500, –510, –520, and –530 mV). (D.) Feedback image of the same area as in B. but in a solution of 2 mM ferrocenemethanol and 0.1 M NaCl at a tip potential of 600 mV vs Ag/AgCl.

potentials, the tip current profile is roughly similar in shape to the *ocp* scan but with a lower overall current. This data indicates that oxygen diminishment is due to electron transfer and not to a chemical reaction at the surface of the composite. In addition, diminishment of oxygen concentration at *ocp* implies a local cathode to supply the reduction current.

The hypothesis that the SiC particles are the local cathodes is tested by imaging the same region but after replacing the water with a 0.1 M NaCl (pH 6.8) solution containing 2 mM ferrocenemethanol and performing feedback imaging. Figure 3D is the resulting feedback image, which indicates the SiC particles. Comparison of image in 3B and 3D indicates that the SiC particles are the location of oxygen reduction at the surface. Sample topography also affects the oxygen image but the image in Figure 3D indicates that sample topography is only partly responsible for the observed oxygen signal.

Further evidence against sample topography being solely responsible for the oxygen image is found in the images of Figure 4. Figure 4A is an SECM image, at a *x*-*y* plane around 5 μm above the composite with a 10 μm diam Pt tip in boric acid/borax buffer. Although poorly resolved, the SiC particles produce a positive feedback signal similar to that found in NaCl solutions and thus SiC is located at the highest current (lightest gray). Subsequently, the variation of the oxygen above the SiC was determined in the same solution by changing the tip potential from 600 to –400 mV. The *ocp* in the boric acid/borax solution was –550 mV vs Ag/AgCl, which is sufficient to reduce dissolved oxygen. Oxygen depletion above the SiC is found in the vertical (*y*-*z* plane) scan of Figure 4B. A scan at $x = 25$ μm (white dashed line on Figure 4A) shows the oxygen concentration is depleted (lighter color) well above the surface of the SiC particle, as

expected for localized reduction of oxygen.

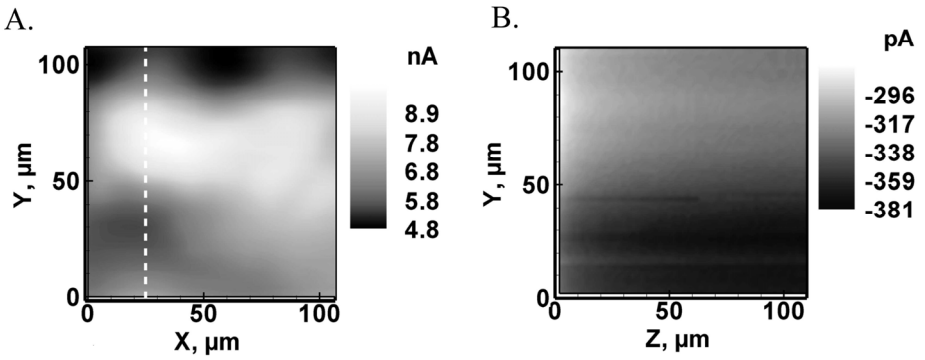

FIGURE 4. SECM images of the composite immersed in boric acid/borax buffer (pH 6.8) containing 2 mM ferrocenemethanol at a 10 µm diam Pt tip. The substrate was kept at *ocp* during the experiments (550 mV vs. Ag/AgCl). (A.) SECM image parallel to the substrate (*x*-*y* plane) with the tip biased at 600 mV vs. Ag/AgCl. (B.) SECM image perpendicular to the substrate (*y*-*z* plane) through the white dashed line in A. with a tip biased at –400 mV vs. Ag/AgCl.

CONCLUSIONS

The results of this study demonstrate that SECM is useful in imaging variations in electrochemical activity over the surface of metal matrix composites in contact with buffered or unbuffered chloride-containing neutral solutions.

SECM imaging using ferrocenemethanol as a redox mediator in a 0.1 M NaCl solution and in a buffer solution (pH 6.8) revealed that the SiC particles are electrochemically active. The data suggests that the electronic conductivity at these sites is higher than that of the Al_2O_3 film covering the alloy matrix surface.

SECM measurements, using oxygen as a mediator in deionized water and in the buffer solution (pH 6.8) showed that the oxygen reduction reaction took place at the surface of the composite, preferentially at the location of the SiC particles.

In future work, we wish to further explore the role of the aluminum in the corrosion

of SiC_p/Al MMCs. One approach is to alter the thickness and hydration of the oxide-layer and the alloy composition and, thus, change the electronic defect density of the of the oxide film.

ACKNOWLEDGEMENTS

The authors would like to acknowledge the National Science Foundation for its support by the grant DBI-9987028. L. D. also wants to express his thanks to CONACYT for his financial support during his sabbatical period.

REFERENCES

1. D. Weiss, B. Chamberlain and R. Bruski, *Modern Casting*, **58**, 58 (2000).
2. M. J. Kocjak, S. C. Kahtri, J. E. Allison and J. W. Jones, in *Fundamentals of Metal-Matrix Composites*, S. Suresh, A. Mortensen and A. Needleman, Editors, p. 297, Butterworth-Heinemann, Stoneham, MA, (1993).
3. M. Occhionero, R. W. Adams, K. P. Fennnessy and R. A. Hay, in *Aluminum Silicon Carbide (AlSiC) Thermal Management Packaging For High Density Packaging Applications*, p. 1, International Microelectronics and Packaging Society, Denver CO, (1999).
4. C. Zweben, *JOM*, **7**, 15 (1992).
5. M. I. Pech-Canul, R. N. Katz and M. M. Makhlouf, *J. Mater. Process. Technol.*, **108**, 68 (2000).
6. M. A. Pech-Canul, M. I. Pech-Canul, M. Echeverría and S. D. Córdova-García, in

Proceedings of the 15th International Corrosion Congress on Frontiers in Corrosion Science and Technology, paper #612, Granada, Spain, (2002).

7. Z. Ahmad and B. J. A. Aleem, *Mater. Design*, **23**, 173 (2002).
8. G. E. Kiourtsidis, S. M. Skolianos and E. G. Pavlidou, *Corros. Sci.*, **41**, 1185 (1999).
9. H. J. Greene and F. Mansfeld, *Corrosion*, **53**, 920 (1997).
10. P. C. R. Nunes and L. V. Ramanathan, *Corrosion*, **51**, 610 (1995).
11. C. Monticelli, F. Zucchi, F. Bonollo, G. Brunoro, A. Frignani and G. Trabanelli, *J. Electrochem. Soc.*, **142**, 405 (1995).
12. J. E. Castle, L. Sun and H. Yan, *Corros. Sci.*, **36**, 1093 (1994).
13. L. H. Hihara and R. M. Latanison, *Corrosion*, **48**, 546 (1992).
14. http://www.hexoloy.com/sa/reference.html, in *Hexoloy SA Typical Physical Properties*, Saint-Gobain Advanced Ceramics, (2002).
15. H. Jeong, *Res. Nondestr. Eval.*, **9**, 41 (1997).
16. A. J. Bard, F.-R. F. Fan, J. Kwak and O. Lev, *Anal. Chem.*, **61**, 132 (1989).
17. J. Kwak and A. J. Bard, *Anal. Chem.*, **61**, 1221 (1989).
18. A. J. Bard, in *Scanning Electrochemical Microscopy*, A. J. Bard and M. V. Mirkin, Editors, p. 1, John Wiley & Sons, New York, (2001).
19. D. O. Wipf and A. J. Bard, *J. Electrochem. Soc.*, **138**, L4 (1991).
20. D. O. Wipf and A. J. Bard, *J. Electrochem. Soc.*, **138**, 469 (1991).

21. L. Veleva, L. Díaz-Ballote and D. O. Wipf, *J. Electrochem. Soc.*, **150**, C1 (2003).

22. J. L. Gilbert, S. M. Smith and E. P. Lautenschlager, *J. Biomed. Mater. Res.*, **27**, 1357 (1993).

23. J. L. Gilbert, L. Zarka, E. B. Chang and C. H. Thomas, *J. Biomed. Mater. Res.*, **42**, 321 (1998).

24. B. Liu, W. Cheng, S. A. Rotenberg and M. V. Mirkin, *J. Electroanal. Chem.*, **500**, 590 (2001).

25. J. C. Seegmiller and D. A. Buttry, *J. Electrochem. Soc.*, **150**, B413 (2003).

26. M. I. Pech-Canul, R. N. Katz and M. M. Makhlouf, *Metall. Mater. Trans. A*, **565**, 31A (2000).

27. R. M. Wightman and D. O. Wipf, in *Electroanalytical Chemistry*, A. J. Bard, Editor, Vol. 15, p. 267, Marcel Dekker, New York, (1989).

28. F.-R. F. Fan and C. Demaille, in *Scanning Electrochemical Microscopy*, A. J. Bard and M. V. Mirkin, Editors, p. 75, John Wiley & Sons, New York, (2001).

29. M. Pourbaix, in *Atlas of Electrochemical Equilibria in Aqueous Solutions*, p. 99, NACE-Cebelcor, Houston, (1974).

30. I. Serebrennikova and H. S. White, *Electrochem. Solid-State Lett.*, **4**, B4 (2001).